Pergamon
www.elsevier.nl/locate/asr

Adv. Space Res. Vol. 26, No. 10, pp. 1477–1488, 2000

Printed in Great Britain
0273-1177/00 $20.00 + 0.00

PII: S0273-1177(00)00081-8

INFRARED SPECTROSCOPIC STUDIES OF THE JOVIAN IONOSPHERE AND AURORAE

S. Miller[1], D. Rego[1], N. Achilleos[1], T.S. Stallard[1],
R. Prangé[2], M. Dougherty[3], R.D. Joseph[4], J. Tennyson[1],
A. Aylward[1], I. Meuller-Wodarg[1] and D. Rees[5].

[1]*Dept. of Physics and Astronomy, University College London, London WC1E 6BT, U.K.*
[2]*Inst. d'Astrophysique Spatiale, 91405 Orsay Cedex, France*
[3]*Dept. of Space and Atmospheric Physics, Imperial College, London SW7 2BZ, U.K.*
[4]*Inst. for Astrophysics, University of Hawaii, Honolulu HI96822, U.S.A.*
[5]*Center for Atmospheric and Space Sciences, Utah State University, Logan, Utah, U.S.A.*

ABSTRACT

We review recent spectroscopic studies of the ionosphere of Jupiter. These demonstrate the importance of the H_3^+ molecular ion in understanding not only the ion-molecule chemistry of the jovian upper atmosphere, but of its energetics and dynamics as well. Comparisons are made with a new three-dimensional, global circulation model of Jupiter's ionosphere and thermosphere, JIM.

INTRODUCTION

The ionosphere and thermosphere of Jupiter form one of the most dynamic of all the planetary systems we know of. They are coupled to the Jovian magnetosphere, the largest structure in the Solar System with the exception of the Solar Wind. Jupiter's magnetosphere not only picks up energy and charged particles from this wind, in a similar fashion to that of the Earth, but it is also supplied with plasma from within by the volcanic activity of the closest of the Galilean moons, Io. The coupling between the magnetosphere and ionosphere forms a mechanism by which the planet loses rotational energy, driving a series of currents which, in turn, supply heating to the upper atmosphere (Hill, 1979). Although it has been extensively studied and modeled, the jovian ionosphere/thermosphere still presents many unanswered questions, e.g. how to account for its relatively high temperature (see, e.g., Atreya, 1986).

Spectroscopic measurements of the Jovian ionosphere have been carried out ever since the ultraviolet spectrometer on Voyager I first detected aurorae on Jupiter (Broadfoot et al., 1981). In the UV, measurements of the auroral emission due to H Lyman$-\alpha$ and the Lyman and Werner bands of H_2 have been made since the late 1970s (e.g. Clarke et al., 1980; Livengood et al., 1992; Feldman et al., 1993). Hydrocarbon emission from the Jovian auroral regions has also been known from about the same time (Caldwell et al., 1980; Kostiuk et al., 1987). In 1988, the first spectrum of the molecular ion H_3^+ was measured for the first time outside of the laboratory, emanating from Jupiter's aurorae (Drossart et al., 1989). In the decade that has followed, this ion has contributed significantly to our understanding of the morphology and time dependence of Jupiter's aurorae (e.g. Baron et al., 1991; Satoh et al., 1996;), the nature of the jovian magnetic field (Connerney et al., 1993; 1998) and the physical conditions in the auroral ionosphere (e.g. Miller et al., 1990).

This short review complements that to be found elsewhere in this volume (Waite et al., 1998), concentrating on the last aspect of H_3^+'s contribution to our knowledge of the ionosphere of Jupiter. In particular, it makes use of three recent studies which have attempted to address the question of the contribution H_3^+ makes to the energy balance of the Jovian ionosphere/thermosphere (Lam et al., 1997; Miller et al., 1997), the morphology of the ion's emission (Rego et al., 1999a,b) and what it may be telling us about the dynamics of the upper atmosphere of Jupiter (Rego et al, 1999c). It also makes comparisons with studies carried out using the Jovian Ionospheric Model (JIM) (Achilleos et al., 1998).

AURORAL AND IONOSPHERIC ENERGY BALANCE

Two recent studies (Lam et al, 1997 – henceforth Paper I; Miller et al., 1997 – henceforth Paper II) have made use of data obtained on the United Kingdom InfraRed Telescope (UKIRT) on Mauna Kea, Hawaii, to look at the planetwide behaviour of H_3^+ on Jupiter. This telescope has a facility long-slit spectrometer, CGS4, which can be used in grating mode to give spectral resolutions of $\lambda/\Delta\lambda > 1000$. Strong H_3^+ emission may be seen in the 3 to 4 micron L and L' windows from Jupiter's aurorae (Maillard et al., 1990; Miller et al., 1990). Ballester et al. (1994) have also shown that for wavelength settings around 3.2μm to 3.7μm, H_3^+ emission lines could be detected at all latitudes at intensities great enough to enable temperatures and column densities to be fitted (Figure 1). This opened up the prospect of making use of H_3^+ to answer some of the outstanding questions concerning the entire jovian ionosphere.

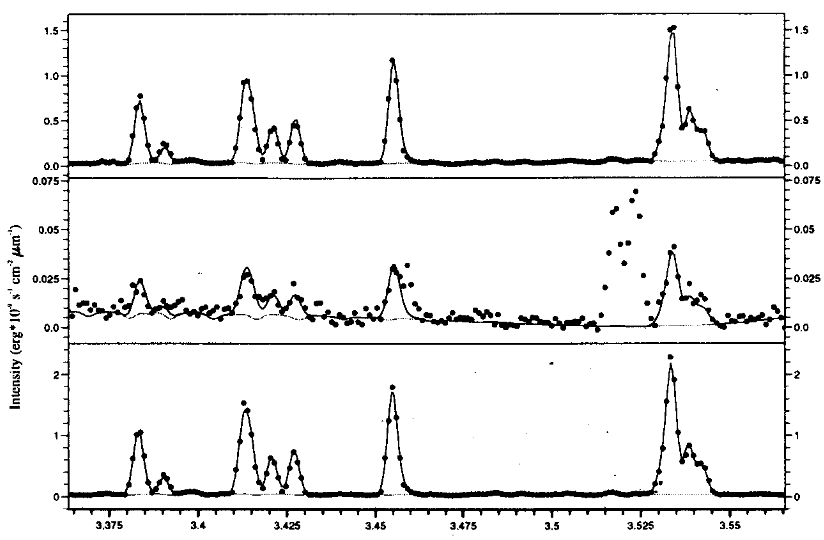

Figure 1. Typical H_3^+ spectral fits to the 3.47μm spectra of Jupiter for the 1993 UKIRT data of Lam et al. (1997). Filled circles, observed spectrum; solid line, fit; broken line, continuum contribution. Top, northern auroral zone; middle, equatorial region; bottom, southern auroral zone. H_3^+ emission accounts for all the observed spectrum in the auroral zones. At the equator, there is a doublet at 3.52μm due to reflected solar IR.

Paper I reported global temperatures that ranged from 800K to >1000K in the auroral regions to 700K to >900K in the equatorial to mid latitudes (Figure 2). Corresponding column densities were a few $\times 10^{16}$ m^{-2} for the aurorae going down to $< 10^{15} m^{-2}$ for the equatorial region (Figure 3). The planetary temperatures indicated structure in the latitudinal profile, with high temperatures in the aurorae followed by cooler mid-latitudes and a return to higher temperatures in the equatorial region (Fig. 2). While confirming the general structure reported in Ballester et al. (1994) for the one central meridian longitude (CML) ($\lambda_{III} = 102°$) investigated there, Paper I did, however, conclude that their very high equatorial temperatures – >1200K – were an artifact of a poor approximation to the continuum. The temperature structure is consistent with the notion that, in the auroral zones, high temperatures are produced by the energy deposited by particle (mainly kev electron) precipitation.

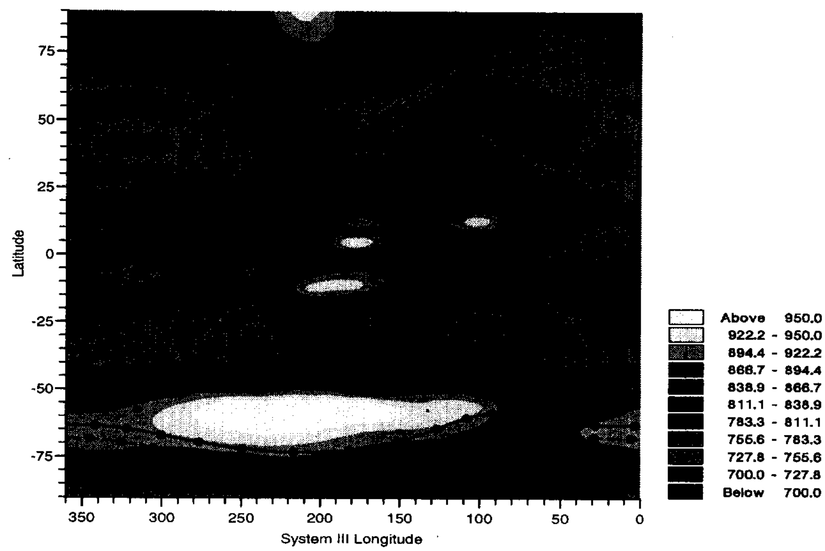

Figure 2 H_3^+ temperature map of Jupiter derived from the 1993 UKIRT data of Lam et al. (1997).

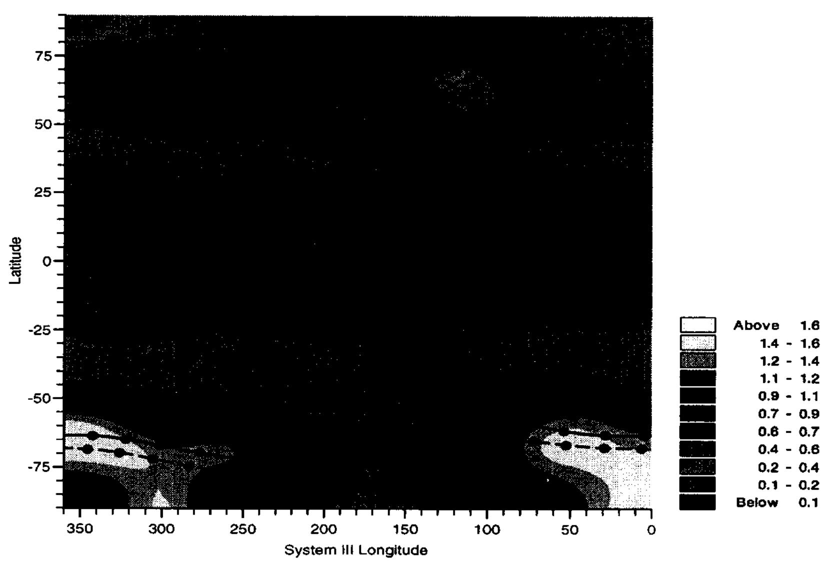

Figure 3. H_3^+ column density map of Jupiter derived from the 1993 UKIRT data of Lam et al. (1997). The units are $10^{16} m^{-2}$.

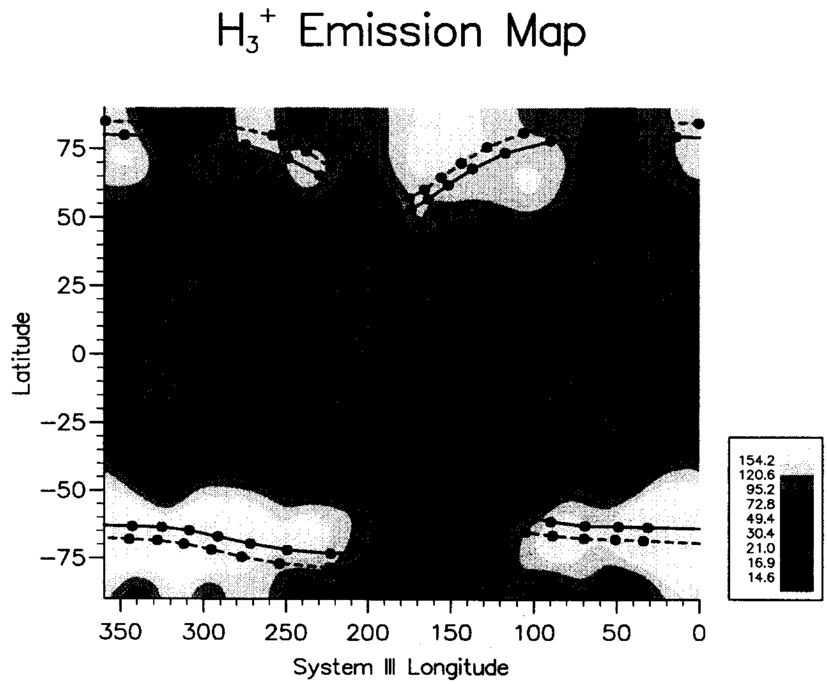

Figure 4. H_3^+ emission map of Jupiter derived from the 1993 UKIRT data of Lam et al. (1997). The units are mW $m^{-2}sr^{-1}$.

One important point to emerge in Paper I was that it was very difficult to fit temperatures and column densities independently, since these parameters turned out to be more than 90% anti-correlated. So the authors introduced a parameter $E(H_3^+)$, which represented the energy emitted by H_3^+ over its entire spectral range (see Paper I for more details) (Figure 4). This parameter proved to be invaluable in calculating the contribution of the H_3^+ to the energy budget of Jupiter's upper atmosphere. In the auroral regions, Paper I showed that the total H_3^+ emission was of the order of 3×10^{12} Watts per hemisphere, making its effect comparable to – if a little less than – that of the ultraviolet aurorae (see Livengood et al., 1992). In the non-auroral regions, H_3^+ was found to be emitting of the order of 0.1mW m^{-2} even at the equator, with higher amounts found at higher, but sub-auroral, latitudes. This amount was greater than the solar influx of extreme-UV (EUV) photons, available to produce ionisation, and added to the problem of how to account for the high temperature of the jovian thermosphere (see Atreya 1986). The importance of H_3^+ as an ionospheric coolant was emphasised by Waite et al. (1997), who found that the Galileo temperature profiles could not be fitted without including this contribution to the energy balance.

Paper II considered two possibilities to account for the high emission of H_3^+in the non-auroral regions: additional mid-to-low latitude particle precipitation – presumably from the radiation belts inside the orbit of Io – and transport of ions and/or energy from the auroral regions by winds. The authors were not able to rule out either possibility, although the structure of the emission (Fig. 4) suggested particle precipitation might be the more important contribution, an idea borne out by fitting recent X-ray data (Waite et al., 1997). Overall Papers I and II showed that models of the jovian thermosphere would not be able to represent the energy balance correctly unless the cooling effect of H_3^+ were taken into account, along with its contribution to the chemical processes occurring there.

HIGH RESOLUTION LATITUDINAL PROFILES

The spatial resolution available on CGS4 at the time the data for Papers I and II were obtained (May 3 to 5, 1993) was limited to a 3.1" x 3.1" pixel, which corresponded to almost 10,000km on the plane at Jupiter. This meant that it was not possible to resolve any detail in the auroral regions and that some of the emission reported in the peri-auroral region might have resulted from some "spillage" from pixels covering the aurorae themselves. But better spatial resolution was obtained a few years later (July 11-14, 1996), making use of the facility long-slit echelle spectrometer, CSHELL, on the NASA InfraRed Telescope Facility (IRTF), also on Mauna Kea, Hawaii. CSHELL has a spatial resolution of 0.2", equivalent to <700km at Jupiter at opposition, in the direction along the slit. Using a 1" slit, which gave $\lambda/\Delta\lambda > 20,000$, H_3^+emission could also be detected at all latitudes at wavelengths as long as 4.1μm (Rego et al., 1999a – henceforth Paper III). In particular the ν_2 Q(1,0$^-$) line at 3.953μm turned out to be a very good probe of the latitudinal emission profile; secondary use could be made of the Q(3,0$^-$) line at 3.986μm, particularly for probing the temperature structure of the planet.

Paper III set out to look at the H_3^+ emission profile in detail with a view to answering the questions raised in Papers I and II. The authors reasoned that particle precipitation would not occur at the magnetic equator of the planet, where the dip angle was – by definition – zero. They therefore took the H_3^+emission observed at these equatorial latitudes to be the result of ions produced by solar EUV ionisation, assuming that transport of auroral H_3^+ would be negligible for this region. (At the electron densities prevailing in the non-auroral ionosphere – $10^9 - 10^{10}$m^{-3} – the H_3^+ lifetime is $10^3 - 10^4$ seconds, which would require meridional windspeeds of several km/s to transport significant quantities of the aurorally produced H_3^+ to the equator. There is no direct observational evidence for such winds, as yet.) They then modeled the latitudinal emission profile that solar EUV ionisation would produce. This left clear deficiencies in the auroral and polar regions.

These effects could be modeled by introducing the emission due to a bright narrow auroral oval and a contribution representing the diffuse aurora and local time effects proposed by Satoh et al. (1996) to account for IR images of Jupiter's aurorae. The resulting multi-emission component (MEC) model using the three contributions – EUV, auroral and diffuse/local-time, known as MEC3 – still left emission in the mid-to-low (MTL) latitudes unaccounted for (Figure 5, top). But a four component model, MEC4, which took specific account of the MTL emission, fitted the observed profiles well (Figure 5, bottom). In MEC4, the MTL contribution was represented by a component which commenced in a step-wise fashion at the lowest latitude of the auroral component and declined exponentially as a function of decreasing latitude; a constant component which fitted the lowest latitudes for which MTL emission was observed, severely underestimated the peri-auroral emission even when convolved with the line-of-sight effect.

In Figure 6 we plot the locations and extent of the auroral, diffuse and MTL as a function of CML. (N.B. at some longitudes, the fitted auroral components is at such high latitude that it is not possible to separate it from the diffuse component. Then, only the auroral component, which may contain a contribution from the diffuse emission, is plotted.) The locus of the auroral oval produced by the MEC4 fit corresponded well with that deduced from UV observation using the Hubble Space Telescope's WFPC2 camera (Clarke et al., 1996; Ballester et al. 1996) for the northern hemisphere, although the correspondance was less good in the (more problematic) south (Figure 7).

Although the auroral and diffuse components are spatially localised, they contribute between one and

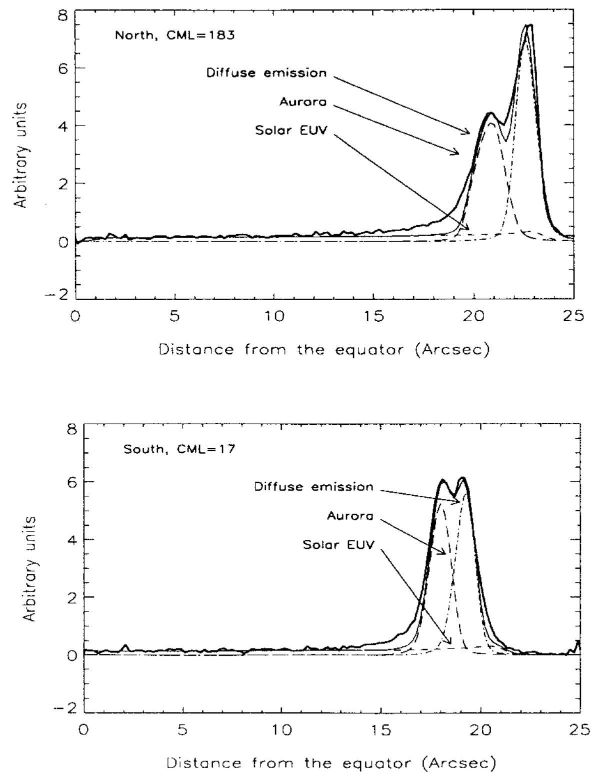

Figure 5. Typical jovian H_3^+ latitudinal intensity profile for the 1996 IRTF data taken at 3.953μm. Thick line, observed profile; thin line, fitted profile; long-dash line, auroral emission; dot-dash line, diffuse emission; short-dash line, EUV component. Top: fit with the MEC3 model. The fit is poor between 13" and 17", corresponding to the mid-to-low latitudes. Bottom: fit with the MEC4 model. The fit is now almost perfect.

fourteen times the total emission due to EUV-produced H_3^+, dependent on CML. It is also noticeable that the MTL component appears to be a fairly constant proportion of that due to auroral and diffuse emission – between 10% and 25% – even though, for the CMLs measured, it varies between 20% and and 300% of the EUV contribution(Figure 7). This suggests that the MTL component is intrinsically linked to aurorally (narrow or diffuse) produced H_3^+ emission.

The MEC4 model represents a significant advance over the work of Papers I and II, in terms of understanding the latitudinal emission profiles of H_3^+, since it separates the MTL emission from that which can be produced by solar EUV alone. The use of an exponential to represent the MTL component suggests that a "lifetime-governed" process might be at work, in turn suggesting that transport of aurorally produced H_3^+, coupled with the natural decay of the ion due to dissociative recombination, might account for the observed profiles. But the data are not sufficiently sensitive to the exact choice of function to represent the MTL component to rule out other functional forms that might represent the profile which could be obtained if particle precipitation were responsible for this emission. Indeed, in the absence of evidence for fast meridional winds, low-latitude, low-flux particle precipitation still appears to be the more likely candidate to produce the observed H_3^+; the link between the MTL component and the strength of narrow-plus-diffuse auroral components would then suggest that our data monitor effects that may be occuring globally throughout the jovian magnetosphere.

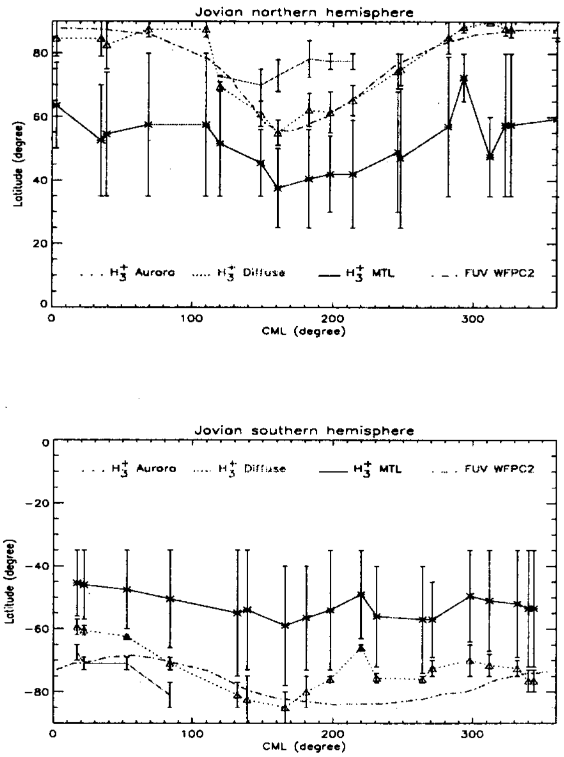

Figure 6. Central location and extent of the auroral, diffuse and MTL components of the MEC4 model fit to the 1996 IRTF latitudinal profiles.

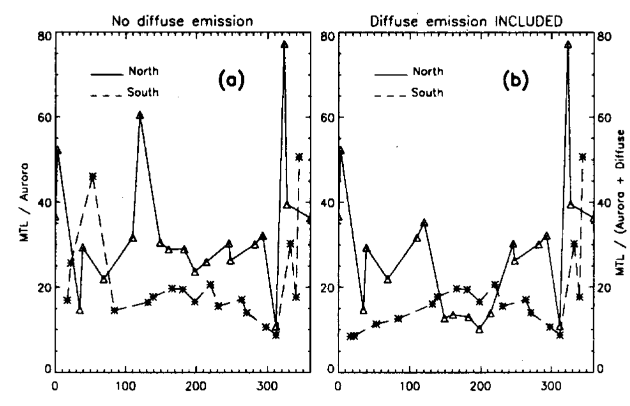

Figure 7. Ratio of MTL component to the auroral and auroral-plus-diffuse components as a function of CML. The components are for the MEC4 model fit to the 1996 IRTF latitudinal profiles.

The data obtained in July 1996 also made it possible to look in more spatial detail at some of the other effects found in Papers I and II. In particular, by comparing the emission obtained from $Q(1,0^-)$ to $Q(3,0^-)$, it was possible to look at the jovian temperature structure once more (Rego et al, 1999b – henceforth Paper IV). This paper found that the general structure – hot auroral regions, cooler mid latitudes and hotter equatorial regions – was reproduced. But it did not find evidence for the "warm channel" found in Papers I and II, running north-south across the planet between longitudes 170° to 210°. (The authors of Paper II suggested that this feature might have corresponded to the fast meridional wind required by Sommeria et al.'s (1995) explanation for the Lyman-α Bulge (Clarke et al., 1980).) But the auroral emission appeared to be more variable on a day-to-day basis in July 1996 than it had been in May 1993, and it may be that these more subtle features were masked by this variability.

AURORAL ELECTROJETS

Although the work reported in Paper IV could not confirm the existence of a hot channel which might correspond with the Sommeria neutral winds, new evidence has come to light that fast – supersonic – ion winds can be produced in the jovian auroral regions. During August, 1997, observations were made on the IRTF in support of the Galileo C9 orbit. Figure 8 compares CSHELL north-south profiles obtained in July 1996 with those obtained on August 8, 1997, for CMLs between 260° and 280° in both the northern and southern hemisphere. The July 1996 data show one bright peak in the H_3^+ emission, corresponding to the CSHELL slit cutting across a single narrow auroral peak. But the August 8, 1997, data showed that this single peak was replaced by a double peak in the north and a peak/tail structure in the south. Images taken in CSHELL imaging mode indicate (the CSHELL imager has a variable wavelength across the array, so are good only for general features, not detailed morphology) that a double arc was present on August 8, 1997.

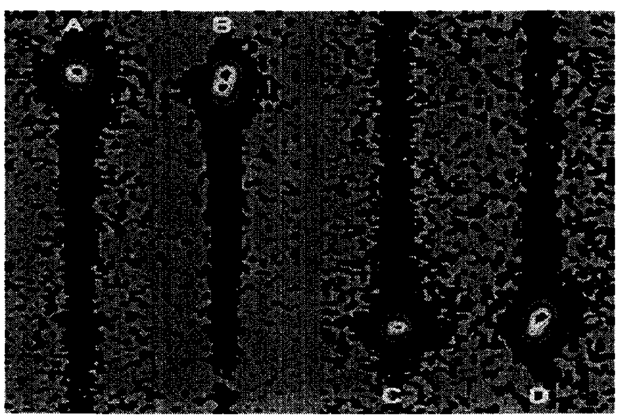

Figure 8. IRTF spectral images obtained at 3.953μm: (A) northern hemisphere, July 16, 1996, 09:56U.T., CML=248°; (B) northern hemisphere, August 8, 1997, 08:55U.T., CML=264°; (C) southern hemisphere, July 14, 1996, 08:46U.T., CML=264°; (D) southern hemisphere, August 8, 1997, 09:05U.T., CML=270°. For each spectral image, wavelength increases left-to-right, and north is at the top. In each case, the spectral image covers the CML from pole to equator.

The general structure outlined aboved persisted for over an hour. Not only that, but the outer structures were clearly wavelength shifted compared with H_3^+ emission from the body of the planet – a shift that was borne out by comparison with lines due to the Earth's sky emission. Generally, an S-shaped profile was produced in velocity space, with the northern outer peak red-shifted by 2.0km/s and the southern tail blue-shifted by about 2.0km/s (Figure 9). Rego et al. (1999c – henceforth Paper V) interpreted the data as the CSHELL slit cutting across electrojets flowing clockwise (counter-rotationally) along auroral ovals close to the 30R_J magnetic fieldline footprints, with some indication of counter-clockwise flows along the lower latitude arcs. After the line-of-sight

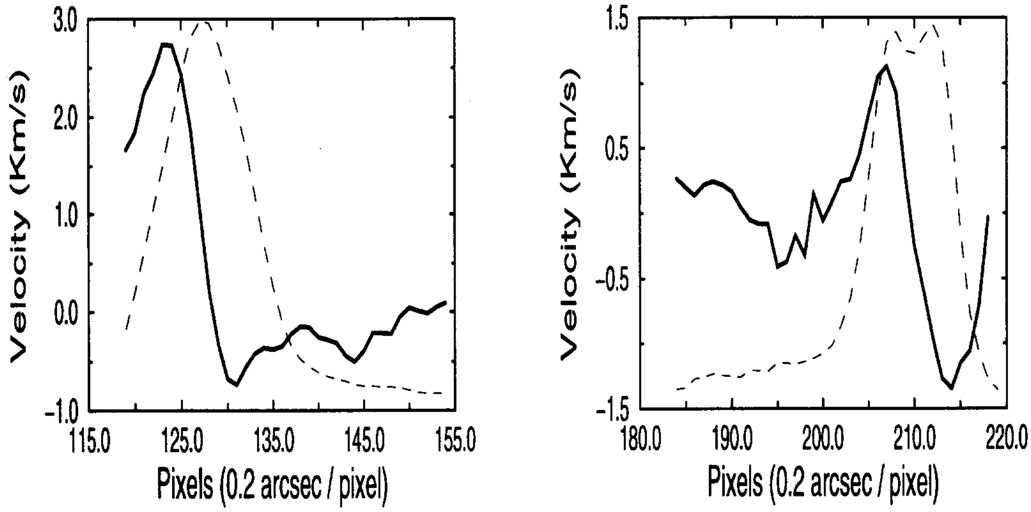

Figure 9. Typical velocity profiles the southern (left) and northern (right) auroral zones. Full line, velocity; dashed line, intensity (arbitrary units). Errors on the velocities are ±0.3km/s.

effect was taken into account, the velocities were 2.7km/s (+/-0.4km/s) for the northern outer peak and 2.9 km/s (+/-0.4 km/s) for the southern tail – in excess of the local speed of sound (2.4km/s).

COMPARISON WITH JOVIAN IONOSPHERIC MODEL

Auroral electrojets in the jovian ionosphere can now be modelled using the UCL Jovian Ionospheric Model (JIM: Achilleos et al., 1998). This model has, amongst its other inputs, a variable potential difference across an auroral region delimited by the footprints of the magnetic field lines which cross the jovian equatorial plane at $6R_J$, at the low-latitude boundary, and $30R_J$, at the poleward boundary (Connerney, 1993). The latitudes spanned by these footprints cover 5000km along the meridian. (Actually, the exact footprints used follow the $7R_J$ and $15R_J$ footprints in the Offset Tilted Dipole model (Acuna et al., 1983), programmed in for its simplicity.) The model also has a constant polar cap potential (Earth-like) of 10^5 Volts. In Figure 10, we show the ion and neutral winds produced around the northern polar/auroral region at the 0.1microBar pressure level (the level of peak H_3^+ production in the auroral regions) for a variety of trans-auroral potentials.

When the trans-auroral potential is 10^4V, winds in the polar/auroral region are dominated by the trans-polar potential, for the ions, and are rotationally and solar driven, for the neutrals. Windspeeds are typically of a few metres/second, rising to 10m/s for the transpolar ions. At 10^5V, the ions are subject to an electrojet of 10m/s, while the neutrals remain essentially indifferent. But at 2×10^6V the ions are subject to an electrojet in excess of 800m/s, while collisions between ions and neutrals impose on the latter an electro-jet orientated wind of 200m/s, some 25% of the ion speed. The kinetic energy tied up in this electrojet may be calculated from the neutral speeds to be of the order of 8×10^{15} Joules per hemisphere. If just 0.1% of this energy is dissipated per second into the surroundings by "frictional" forces, this would add nearly 10^{13}W to the input to the jovian atmosphere per hemisphere, almost an order of magnitude more than the energy input due to solar EUV. Modelling the dissipation of the electrojet energy due to "frictional" forces at the horizontal boundary of the non-auroral and auroral atmosphere is continuing. But with such large amounts of

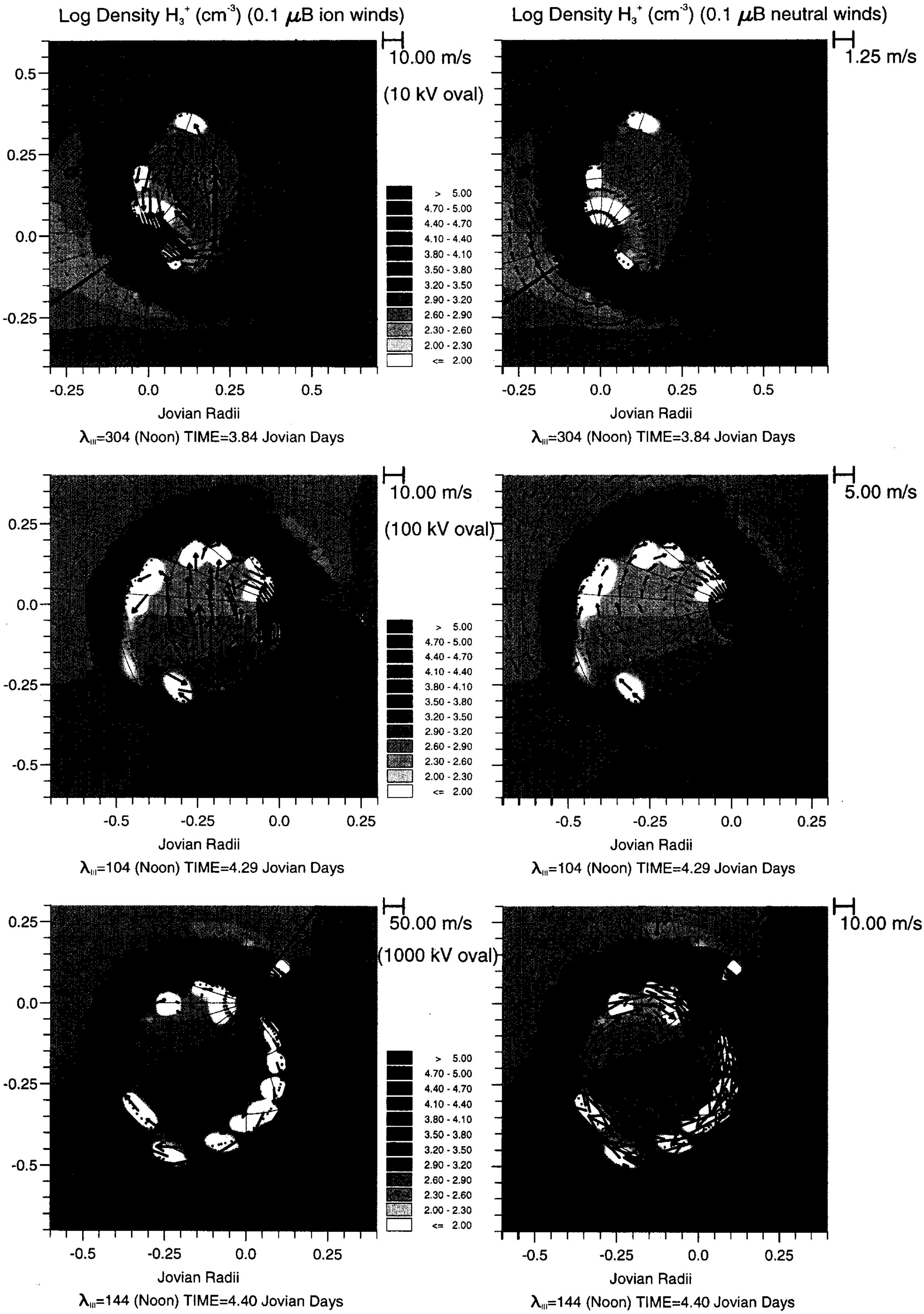

Log Density H_3^+ (cm^{-3}) (0.1 μB ion winds)
Log Density H_3^+ (cm^{-3}) (0.1 μB neutral winds)
10.00 m/s
(10 kV oval)
1.25 m/s
> 5.00
4.70 - 5.00
4.40 - 4.70
4.10 - 4.40
3.80 - 4.10
3.50 - 3.80
3.20 - 3.50
2.90 - 3.20
2.60 - 2.90
2.30 - 2.60
2.00 - 2.30
<= 2.00
Jovian Radii
λ_{III}=304 (Noon) TIME=3.84 Jovian Days
10.00 m/s
(100 kV oval)
5.00 m/s
λ_{III}=104 (Noon) TIME=4.29 Jovian Days
50.00 m/s
(1000 kV oval)
10.00 m/s
λ_{III}=144 (Noon) TIME=4.40 Jovian Days

energy available, it would be surprising if this source did not make some contribution to the thermal balance of the ionosphere/thermosphere, and aacount for at least some of the energy radiated by H_3^+.

CONCLUSIONS

This brief review of recent developments in the IR spectroscopy of the jovian ionosphere shows the importance of the H_3^+molecular ion in understanding not only the ion-molecule chemistry of the upper atmosphere, but the energetics and dynamics as well. In years to come, we anticipate that similar studies will be routine not just for Jupiter, but for the other giant planets as well.

ACKNOWLEDGMENTS

It is a pleasure to acknowledge the assistence of the expert staff at UKIRT and IRTF, without whose assistance this work would not have been possible. The work was supported by the UK Particle Physics and Astronomy Research Council, the French Conseil Nationale de Reccherche Scientifique and NASA.

Figure 10. Wind speeds and H_3^+ intensities at the 0.1μB pressure level (page facing).

REFERENCES

Acuna, M.H., K.W. Behannon and J.E.P. Connerney, Jupiter's magnetic field and magnetosphere, in *Physics of the Jovian Magnetosphere*, edited by A.J. Dessler, Cambridge University press, pp. 1-50 (1983).

Achilleos N., S. Miller, J. Tennyson, A. Aylward, I. Meuller-Wodarg and D. Rees, JIM: a time-dependent, three-dimensional model of Jupiter's theromosphere and ionosphere, *J. Geophys. Res.*, in press (1998).

Atreya S.K., *Atmospheres and Ionospheres of the Outer Planets*, Springer-Verlag, Heidelburg (1986).

Ballester G.E., S. Miller, J. Tennyson, T.R. Geballe and L.M. Trafton, Latitudinal temperature variations of jovian H_3^+, *Icarus*, **107**, pp. 189-194 (1994).

Ballester G.E. and 21 others, Time-resolved observations of Jupiter's far-ultraviolet aurora, *Science*, **274** pp. 409-413 (1996).

Baron R., R.D. Joseph, T. Owen, J. Tennyson, S. Miller and G.E. Ballester, Imaging Jupiter's aurorae from H_3^+ emissions in the 3-4 micron band, *Nature*, **353**, pp. 539-542 (1991).

Broadfoot A.L., B.R. Sandel, D.E. Shemansky, J.C. McConnerll, G.R. Smith, J.B. Holberg, S.K. Atreya, T.M. Donahue, D.F. Strobel and J.L. Bertaux, Overview of the Vyoager ultraviolet spectrometer results through Jupiter encounter, *J. Geophys. Res.*, **86**, 8259-8284.

Caldwell J.T., A.T. Tokunaga, and F.C. Gillett, Possible infrared aurorae on Jupiter, *Icarus*, **41**, 667-675, (1980).

Clarke J.T., H.A. Weaver, P.D. Feldman, H.W. Moos, W.G. Fastie and C.B. Opal, Spatial imaging of hydrogen Lyman alpha emission from Jupiter, *Astrophys. J.*, **240**, pp. 696-701 (1980).

Clarke J.T. and 20 others, Far-ultraviolet imaging of Jupiter's aurora and the Io "fottprint", *Science*, **274**, pp. 404-408 (1996).

Connerney J.E.P., Magnetic fields of the outer planets, *J. Geophys. Res.*, **98**, pp. 18659-18679 (1993).

Connerney J., R. Baron, T. Satoh and T. Owen, Images of excited H_3^+ at the foot of the Io flux tube in Jupiter's atmosphere, *Science*, **262**, pp. 1035-1038 (1993).

Dessler A., B.R. Sandel and S.K. Atreya, The jovian hydrogen bulge: evidence for co-rotating magnetospheric convection, *Planet. Space Sci.*, **29**, pp. 215-224 (1981).

Drossart P. and 11 others, Detection of H_3^+ on Jupiter, *Nature*, **340**, pp. 539-541 (1989).

Feldman P.D., M.A. McGrath, H.W. Moos, S.T. Durrance, D.F. Strobel and A.F. Davidsen, The spectrum of the jovian dayglow observed at 3A resolution with the Hopkins Ultraviolet Telescope, *Astrophys. J.*, **406**, pp. 279-284 (1993).

Hill T.W., Inertial limit on co-rotation, *J. Geophys. Res.*, **84**, pp. 6554-6558 (1979).

Kostiuk T., F. Espanak and M.J. Mumma, Is ethane varying in the jovian north polar "hot spot", in *Time Variable Phenomena in the Jovian System*, edited by M.J.S. Belton, R.A. West and J. Rahe, pp. 234-241, NASA Washington D.C. (1987).

Lam H.A., N. Achilleos, S. Miller, J. Tennyson, L.M. Trafton, T.R. Geballe and G.E. Ballester, A baseline spectroscopic study of the infrared auroras of Jupiter, *Icarus*, **127**, pp. 379-393 (1997).

Livengood T., H.W. Moos, G.E. Ballester and R. Prangé, Jovian ultraviolet auroral activity, 1981-1991, *Icarus*, **97**, pp. 26-45 (1992).

Maillard J.-P., P. Drossart, J.K.G. Wattson, S.J. Kim and J. Caldwell, H_3^+ fundamental band in Jupiter's auroral zones at high resolution from 2400 to 2900 inverse centimetres, *Astrophys. J.* **363**, pp. L37-41 (1990).

Miller S., R.D. Joseph and J. Tennyson, Infrared emissions of H_3^+ in the atmosphere of Jupiter in the 2.1 and 4.0 micron region, *Astrophys. J.*, **360**, pp. L55-58 (1990).

Miller S., N. Achilleos, G.E. Ballester, H.A. Lam, J. Tennyson, T.R. Geballe and L.M. Trafton, Mid-to-low latitude H_3^+ emission from Jupiter, *Icarus*, **130**, pp. 57-67 (1997).

Rego D., S. Miller, N. Achilleos, R. Prangé and R.D. Joseph, Latitudinal profiles of the jovian IR emissions of H_3^+ at 4 microns with the NASA Infrared Telescope Facility, *Icarus*, submitted (1999a).

Rego D., work in progress (1999b).

Rego D., N. Achilleos, T. Stallard, S. Miller, R. Prangé, M. Dougherty and R.D. Joseph, Supersonic winds in Jupiter's aurorae, *Nature*, **399**, pp. 121-124 (1999c).

Satoh T., J.E.P. Connerney and R.L. Baron, Emission source model of Jupiter's H_3^+ aurorae: a generalized inverse analysis of images, *Icarus*, **122**, pp.1-23, (1996).

Sommeria J., L. ben Jaffel, and R. Prangé, On the existence of supersonic jets in the upper atmosphere of Jupiter, *Icarus*, **119**, pp. 2-25 (1995).

Waite J.H. Jr. G.R. Gladstone, P. Drossart, T.E. Cravens, A Maurellis, W.S. Lewis, B. Mauk and S. Miller, Jovian equatorial X-ray emission: key to understanding high atmospheric temperatures measured by the Galileo probe, *Science*, **276**, pp. 104-108 (1997).

Waite J.H. Jr. et al., *This volume* (1998).